

## Highlights

### **Reducing RES Droughts through the integration of wind and Solar PV**

Boris Morin, Aina Maimó Far, Damian Flynn, Conor Sweeney

- RES droughts are analysed using 45 years of hourly wind and solar PV generation data
- RES droughts from C3S-Energy and ERA5-Atlite datasets are compared
- Adding solar PV to a wind-dominated system reduces RES drought frequency and duration
- Validated RES datasets are crucial to accurately identify RES drought extremes

# Reducing RES Droughts through the integration of wind and Solar PV

Boris Morin<sup>a,\*</sup>, Aina Maimó Far<sup>a</sup>, Damian Flynn<sup>b</sup>, Conor Sweeney<sup>a</sup>

*<sup>a</sup>School of Mathematics and Statistics, University College Dublin, Belfield, Dublin  
4, Dublin, D04 V1W8, Ireland*

*<sup>b</sup>School of Electrical and Electronic Engineering, University College Dublin, Belfield,  
Dublin 4, Dublin, D04 V1W8, Ireland*

---

\*Corresponding author

*Email addresses:* `boris.morin@ucdconnect.ie` (Boris Morin ),  
`aina.maimofar@ucd.ie` (Aina Maimó Far), `damian.flynn@ucd.ie` (Damian Flynn),  
`conor.sweeney@ucd.ie` (Conor Sweeney)

---

## Abstract

Increasing the share of electricity produced from renewable energy sources (RES), combined with RES dependence on weather, poses a critical challenge for energy systems. This study investigates the importance of the balance between wind and photovoltaic (PV) capacity on periods of low renewable generation, known as RES droughts. Three different RES models are used to estimate the capacity factors for different scenarios of installed capacities for wind and solar PV power. The skill of the RES models is quantified by comparing capacity factor time series to observed hourly data and by assessing their representation of observed RES droughts. The RES models are used to generate a 45-year hourly time series of RES capacity factor, enabling analysis of the frequency, duration and return periods of RES droughts at a climatological scale. Results show the importance of using an accurate, validated RES model for RES drought risk assessment. The addition of solar PV capacity to a wind-dominated system results in a significant reduction in the frequency and duration of RES droughts, while also reducing extremes and seasonal drought patterns. These findings underscore the importance of diversification in RES capacity to enhance energy security and resilience.

*Keywords:* RES Drought, Wind Power, Solar PV Power, Renewable Energy Sources, Return Periods

---

## 1. Introduction

The EU aims to generate at least 69% of its electricity from renewable energy sources (RES) by 2030, up from 41% in 2022 [1]. While this transition is essential for reducing greenhouse gas emissions, it also highlights the challenge of managing the variability of weather-dependent energy sources such as wind and photovoltaic (PV) power. This challenge is amplified by the increasing electrification of energy sectors, which places greater demand on the power system and makes it more sensitive to meteorological conditions, both in historical [2] and future climates [3]. Periods of low renewable generation, known as *Dunkelflaute* or RES droughts, pose significant risks to system adequacy and energy security, emphasising the need for a resilient energy system to meet both growing electricity demand and decarbonisation targets.

14 This study focuses on Ireland, a region with a strong reliance on wind  
15 power, which has ambitious targets for solar PV power expansion. This case  
16 study provides valuable insights into the potential benefits of diversifying  
17 the renewable energy mix on RES droughts. The performance of different  
18 RES datasets are compared, and a 45-year time series of RES generation is  
19 produced. The results highlight the role of increased solar PV capacity in  
20 reducing RES drought risks, offering insights for policymakers and energy  
21 planners.

22 For this study, a RES drought event is defined as occurring when the  
23 average capacity factor (CF) remains below a fixed threshold for a given  
24 duration, following the methodology used in previous research. Kaspar et  
25 al. [4] analysed the shortfall risks of low wind and solar PV in Europe, with  
26 a focus on Germany. Mockert et al. [5] expanded on this by examining  
27 the link between weather regimes and RES droughts in Germany. Similar  
28 analyses were conducted using machine learning for Japan [6] and Hungary  
29 [7]. Alternative methods exist for defining RES droughts. One approach uses  
30 relative CF thresholds that adjust throughout the year to account for seasonal  
31 variations in renewable electricity generation. Raynaud et al. [8] defined a  
32 drought as a sequence of days with energy production below a threshold,  
33 applying this method over a number of European regions. This methodology  
34 was later used to study wind and solar PV droughts in India using machine  
35 learning methods [9]. Kapica et al. [10] built upon this approach to compare  
36 the likelihood of RES droughts increasing in Europe under different climate  
37 models. Rinaldi et al. [11] instead defined RES droughts as periods when  
38 wind or solar PV CF falls below a percentage of the daily mean for that time  
39 of year and assessed RES drought risks in the U.S. Western Interconnection.  
40 Also focusing on the U.S., Brown et al. [12] used a weekly timescale rather  
41 than hourly or daily data and examined RES droughts from a meteorological  
42 perspective. Another method defines energy drought indices based on metrics  
43 commonly used in hydro-meteorology to characterise RES droughts [13]. This  
44 approach identifies periods of unusually low generation relative to historical  
45 production levels, using the lowest production percentiles. It has been applied  
46 in other studies, including analyses of RES droughts in the U.S. [14] and  
47 China [15]. In addition to examining periods of low renewable electricity  
48 generation, Raynaud et al. [8] analysed the imbalance between electricity  
49 demand and renewable generation, known as residual load. These events were  
50 studied alongside low-generation periods to assess their correlation. Similar  
51 analyses have been conducted in Europe [13] and the U.S. [14], revealing

52 differing results across regions.

53 In this paper, the focus is exclusively on renewable electricity generation,  
54 and a fixed threshold approach to define RES droughts is used, which facil-  
55 itates consistent inter-comparison between scenarios with different installed  
56 wind and solar PV capacities.

57 RES droughts are identified using onshore wind and solar PV CF time  
58 series. In this study, three different datasets are used, all of which are driven  
59 by ERA5 data [16]. Two of the datasets are part of C3S Energy (C3S-E), an  
60 energy-based operational dataset produced by the EU Copernicus Climate  
61 Change Service [17]. One of the C3S-E datasets provides CF time series  
62 aggregated at the national scale, while the other provides the CF time series  
63 at each grid point, at the ERA5 resolution of  $0.25^\circ$ . The third dataset was  
64 generated using the Atlite model [18], which converts the ERA5 atmospheric  
65 data to a generation time series using specified wind turbine and PV panel  
66 models. Atlite is an open-source tool developed by PyPSA [18] and has been  
67 used for estimating wind and solar PV generation in order to study RES  
68 droughts [5].

69 The aim of this real case study is to answer two questions which could  
70 help on the decision making for the planning of reserve capacity in wind-  
71 dominated renewable energy system

- 72 • What is the impact of selecting different modelling assumptions on the  
73 analysis of RES droughts?
- 74 • How does the integration of solar PV into a predominantly wind-based  
75 system alter the characteristics of RES droughts in a real-case setting?

76 The datasets used in this study are detailed in section 2, which describes  
77 their characteristics and relevance for evaluating RES droughts. Section 3  
78 outlines the RES datasets used to simulate wind and solar PV generation and  
79 provides the methodology for defining and identifying RES drought events,  
80 including the thresholds and metrics applied. In section 4, the datasets are  
81 first verified against observed energy data to assess their accuracy, followed by  
82 an analysis of RES drought occurrences for two scenarios with different ratios  
83 of installed wind to solar PV capacities. Finally, section 5 offers a discussion  
84 of the results in the context of energy reliability and future planning, followed  
85 by the main conclusions and recommendations for further research.

## 2. Data

This study uses publicly available datasets to construct and validate the datasets for estimating the CF of wind and solar PV energy. The primary data sources include: EirGrid and SONI, the transmission system operators (TSO) for the Republic of Ireland and Northern Ireland, respectively; the ERA5 reanalysis dataset; and the C3S-E datasets.

### 2.1. Wind and solar PV Capacity and Availability

EirGrid, the TSO for the Republic of Ireland, and SONI, the Northern Ireland TSO, provide detailed datasets on all wind and solar PV farms across the island of Ireland (Republic of Ireland and Northern Ireland) from 1990 to the present [19]. These datasets include information such as each farm’s installed capacity, name, and connection date. To enhance the accuracy of this data, the longitude and latitude for each farm were manually determined through online searches. For simplicity, this data will be referred to as originating from EirGrid, as all-island data was directly obtained from EirGrid, and the combined regions of the Republic of Ireland and Northern Ireland will be referred to as Ireland throughout the remainder of this document.

The spreadsheet available from the EirGrid website contains two key variables: generation and availability. Generation is the energy that a RES farm actually contributed to the grid, which may include limitations introduced by the TSO to maintain grid stability, such as constraints and curtailment. Availability represents the energy that would have been generated from a RES farm if no grid constraints had been applied, making it representative of the weather-related response. Generation and availability values are available from 2014 onward for wind power and from 2018 onward for solar PV power, although solar PV availability data only became present in the Republic of Ireland in 2023. This study focuses on availability for all analyses.

### 2.2. Atmospheric Variables

Atlite and C3S-E datasets are driven by the ERA5 reanalysis [16], produced by the European Centre for Medium-Range Weather Forecasts (ECMWF). This global gridded dataset provides hourly atmospheric variables from 1940 to the present at a horizontal resolution of  $0.25^\circ$ . It has proven to be the best choice for studying renewable energy in Ireland [20]. Table 1 lists the ERA5 variables used by Atlite and C3S-Energy.

Table 1: ERA5 variables used to calculate wind and solar PV generation

ERA5 name	variable
100 metre zonal and meridional wind speed	$u_{100}, v_{100}$
2 metre temperature	$t2m$
Surface net solar radiation	$ssr$
Surface solar radiation downwards	$ssrd$
Top of atmosphere incident radiation	$tisr$
Total sky direct solar radiation at surface	$fdir$

### 2.3. C3S Energy

The EU Copernicus Climate Change Service developed the C3S-E renewable energy dataset for Europe [17], using ERA5 atmospheric variables and weather-to-energy models. This dataset provides hourly CF for wind and solar PV energy from 1979 to the present. The data are available on the same grid as the ERA5 data, which has a horizontal resolution of  $0.25^\circ$ . The time series are also available for download at two aggregated scales: regional (NUTS 2) and national.

The wind CF in the C3S-E model is calculated using wind speeds at 100 metres ( $u_{100}, v_{100}$ ) and a standard turbine model, the Vestas V136/3450, with a fixed hub height of 100 meters. This choice reflects trends in wind turbine installations and was guided by expert recommendations. Since real-time data on the exact wind turbine fleet across Europe is difficult to obtain, C3S-E assumes a homogeneous distribution of turbines across the ERA5 grid. While this approach does not capture the precise capacity factors reported by grid operators, it provides a well-correlated time series that effectively represents the impact of climate variability on wind power generation. The turbine power curves used in the model are sourced from publicly available databases, ensuring consistency with industry standards. The solar PV CF in the C3S-E model is calculated at the grid level and represents the aggregated output of all solar PV systems within each pixel, rather than a single installation. It is derived from meteorological data, including surface solar radiation downwards ( $ssrd$ ) and air temperature ( $t2m$ ), using a reference solar PV plant model. This model incorporates empirical calculations for key system components such as optical losses, module efficiency, and inverters. The final capacity factor accounts for a mix of module orientations typical for each location [21].

### 147 3. Methods

148 This study uses three datasets to analyse RES droughts across the island  
149 of Ireland. Data downloaded from C3S-E were used to obtain two datasets:  
150 one based on national-level data (C3S-E N), and another on grid-level data  
151 (C3S-E G). The third dataset was computed using the Atlite model (Atlite).

#### 152 3.1. C3S-Energy National

153 For national-level analyses, the aggregated CF time series provided by  
154 C3S-E were used at two levels: Republic of Ireland (NUTS0: IE) and North-  
155 ern Ireland (NUTS2: UKN0). These are based on the assumption by C3S-E  
156 that RES generation occurs at every ERA5 grid point in Ireland. We com-  
157 puted a weighted average of these, based on the installed capacity of each  
158 one, to represent the total CF for Ireland.

#### 159 3.2. C3S-E Gridded

160 The gridded dataset from C3S-E was used to create CF datasets which  
161 account for the location of RES farms in Ireland. A list of the RES farms in  
162 Ireland was compiled, including each farm’s latitude, longitude and installed  
163 capacity. Using these coordinates, the nearest grid point on the C3S-E grid  
164 was identified for each farm. The CF values from the C3S-E dataset corre-  
165 sponding to these grid points were retrieved. A weighted average of the CF  
166 values was calculated, with the installed capacity of each farm serving as the  
167 weight, to construct the CF time series for Ireland. This process resulted in  
168 a time series of RES generation for each energy source (wind and PV) for  
169 Ireland, which takes the location of the RES farms into account.

#### 170 3.3. Atlite

171 Atlite transforms weather data into energy data using the gridded ERA5  
172 data and the locations of existing RES farms, as described in C3S-E G.  
173 ERA5 data for wind speed at 100 metres ( $u_{100}$ ,  $v_{100}$ ) are used to calculate  
174 wind generation, while the ERA5 radiation variables ( $ssr$ ,  $ssrd$ ,  $tisr$ , and  
175  $fdir$ ) and air temperature ( $t2m$ ) are used to calculate solar PV generation.  
176 A key distinction between C3S-E and Atlite lies in their representation of  
177 wind turbines and PV panels. This study identifies the most appropriate  
178 wind turbine power curve to use from the 121 power curves made available  
179 by Renewables.ninja [22]. The selection of a specific wind turbine and PV  
180 panel characteristics is further discussed and explained in section 4.1.



### 181 3.4. *Energy Scenarios*

182 In addition to analysing wind and solar PV generation separately, a com-  
183 bined CF was computed for each dataset by averaging wind and solar PV  
184 generation, weighted by their installed capacities at the end of 2023 (5.9  
185 GW for wind power and 0.6 GW for solar PV power). This configuration  
186 is referred to as the 91W-9PV scenario, reflecting the distribution of 91%  
187 wind and 9% PV capacity. Given that solar PV capacity in Ireland is low in  
188 2023, and to explore how a more balanced distribution of wind and solar PV  
189 capacities might impact RES droughts, this study also considered a second  
190 scenario, referred to as 57W-43PV, where the installed solar PV capacity  
191 is assumed to increase to 8.6 GW, while wind capacity rises to 11.45 GW.  
192 These values are based on targets outlined in the roadmap published by the  
193 2024 Climate Action Plan [23]. This study does not include offshore wind in  
194 the analysis. Recent reports suggest that even by 2030, Ireland is unlikely to  
195 have any significant new offshore wind farms, with projected offshore capacity  
196 expected to remain near zero using realistic scenarios [24].

197 New time series were generated for both the Atlite and C3S-E G solar  
198 PV datasets, incorporating a revised distribution of installed capacity across  
199 Ireland as specified in the roadmap. For wind power, the CF time series  
200 remains unchanged, as significant shifts in the location of wind farms are not  
201 expected. In total, twelve CF time series were analysed in this study, six for  
202 individual wind and solar PV CF (three datasets for each source) in the 91W-  
203 9PV scenario, and an additional six time series that include the combined  
204 CF for 91W-9PV and 57W-43PV scenarios across the different datasets.

205 It is important to note that the specific capacity values used in this study  
206 are illustrative and are not intended to reflect precise future realities. Instead,  
207 they serve to explore the impact of transitioning from a wind-dominated sys-  
208 tem (91W-9PV) to a more evenly distributed system (57W-43PV). This ap-  
209 proach allows for a comparative analysis between the two scenarios, assessing  
210 how the balance of RES capacity affects the occurrence of RES droughts.

### 211 3.5. *RES Drought Definition*

212 In this study, a RES drought event was defined as occurring when the  
213 24-hour moving average of CF remains below a fixed threshold of 0.1 for  
214 a period of longer than 24 hours. The choice of this threshold is somewhat  
215 arbitrary, but aligns with similar studies on low renewable energy production  
216 [4, 6, 7]. By using a 24-hour moving average, fewer but longer-lasting events  
217 were captured compared to using the raw CF time series, which can be more

218 sensitive to short-term fluctuations. A fixed threshold approach was chosen  
 219 in this study to enable consistent inter-comparison between datasets.

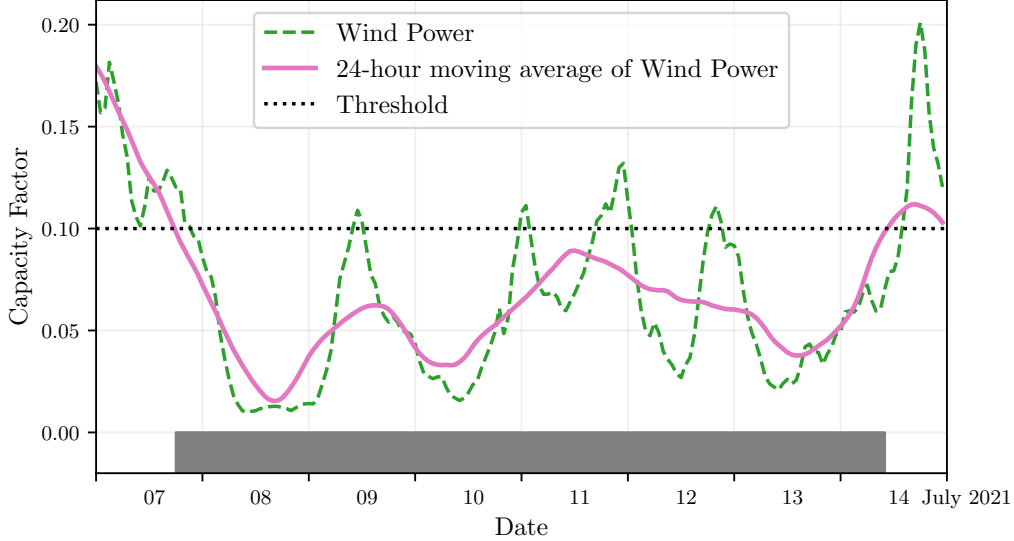


Figure 1: Wind time series of CF (green) and its 24-hour moving average (pink) from the 7th to the 15th of July 2021. The black dashed line indicates the CF threshold. The grey bar shows the period identified as a wind drought under our definition

220 The moving average approach smooths out short-term fluctuations, so  
 221 that brief periods above the threshold do not interrupt an otherwise con-  
 222 tinuous low-CF period (Fig. 1). This means that a single hour above the  
 223 threshold does not "break" a drought event if it is surrounded by prolonged  
 224 low-generation hours. As a result, fewer but longer-lasting drought events  
 225 are identified, which may better reflect real-world conditions where energy  
 226 supply constraints persist over extended periods.

## 227 4. Results

### 228 4.1. Verification

229 The accuracy of the datasets used in this study was verified, before con-  
 230 tinuing to the analysis of RES droughts. For the verification process, time-  
 231 varying values of installed capacity were used to account for changes in RES  
 232 development over the verification period. This step allowed us to assess how

233 well the datasets represent the production of renewable energy by comparing  
 234 them against observed data.

#### 235 4.1.1. Wind Energy

236 The C3S-E datasets use the Vestas V136/3450 wind turbine power curve,  
 237 (Fig. 2a). The Atlite model allows the user to specify the power curve.  
 238 We considered the 121 power curves available for download from Renew-  
 239 ables.ninja [22]. For each power curve, Renewables.ninja also provides four  
 240 associated smoothed power curves. The smoothing is done using a Gaussian  
 241 filter with different standard deviations that depend on the wind speed. A  
 242 separate wind CF time series for Ireland was generated for each of the wind  
 243 turbine power curves and smoothing levels.

244 The performance of each CF time series is then assessed based on four skill  
 245 scores: correlation coefficient (CC), root mean square error (RMSE), mean  
 246 bias error (MBE), and the percentage of overlap. The percentage of overlap  
 247 quantifies the similarity between the observed and modelled distributions. It  
 248 is a positively oriented skill score, where 100% shows full agreement between  
 249 the two distributions, and 0% indicates no overlap. The histograms of hourly  
 250 CF values for the most recent decade (2014-2023) are used to calculate this  
 251 skill score.

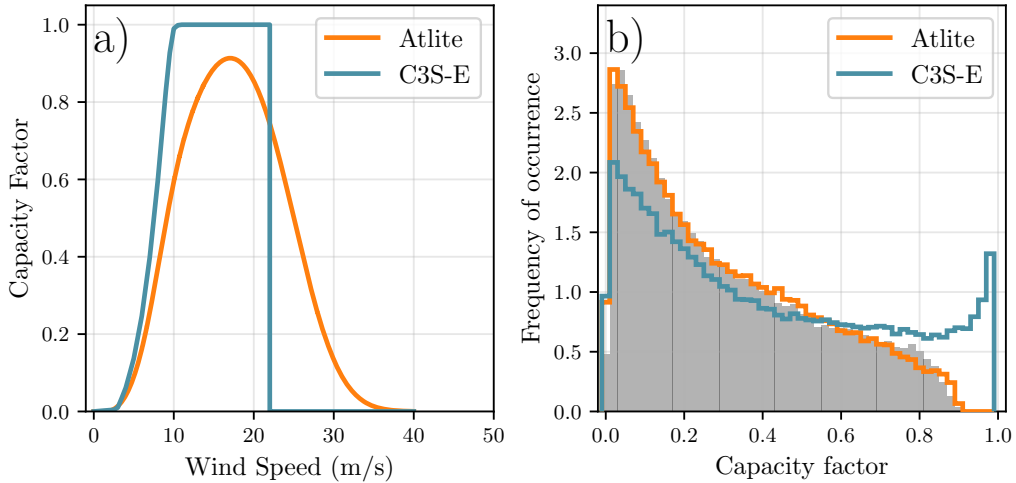


Figure 2: a) Power curves of the Enercon E112.4500 with a 0.3w smoothing filter used by Atlite (orange) and the Vestas V136/3450 used by C3S-E (blue) b) Histograms of wind CF for Ireland from Atlite (orange), C3S-E (blue) and Observed (shaded)

Based on these metrics, the most representative power curve for Ireland is the Enercon E112.4500 power curve with the  $0.3w$  smoothing filter. The smoothing of the wind turbine power curve represents losses associated with each turbine, as well as losses such as wake effects between turbines, which are important when modelling wind energy on larger spatial scales. The histogram in Fig. 2b shows that the C3S-E power curve tends to underestimate low CF values and overestimate higher ones, whereas the smoothed Atlite power curve more closely follows the observed wind availability data. This is further supported by the percentage of overlap which is higher for Atlite (97.2%) than for C3S-E (83.2%), indicating better agreement with observed data.

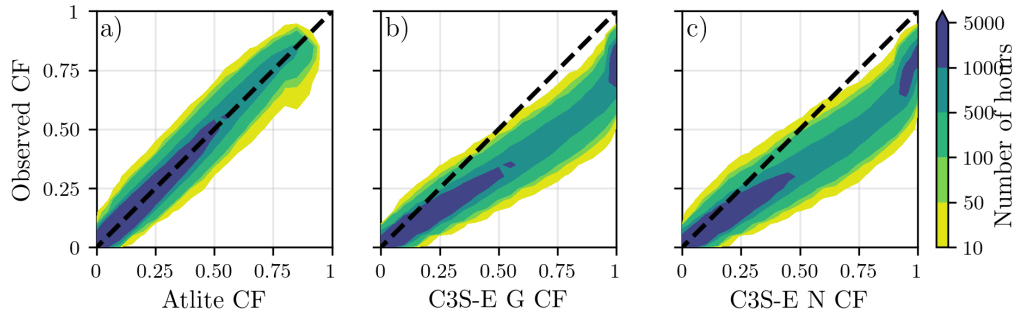


Figure 3: Wind CF density plot of the observed CF (vertical axes) and modelled (horizontal axes) CF data for the a) Atlite, b) C3S-E G and c) C3S-E N datasets

The effect of the difference between the power curves is also visible in Fig. 3, which shows a density plot of wind CF values. The two C3S-E datasets are shown to overestimate the observed CF, whereas the Atlite model is in good agreement with the observed data. The skill scores presented in Table 2 show that Atlite performs better than the C3S-E datasets for all of the skill scores.

	Atlite	C3S-E G	C3S-E N
<b>CC</b>	0.981	0.972	0.970
<b>RMSE</b>	0.045	0.177	0.162
<b>MBE</b>	-0.003	0.137	0.121

Table 2: Skill scores for wind power for the three datasets compared to observed data

Fig. 4 shows the average annual number of wind drought events during

270 the 2014 to 2023 validation period. The figure reveals that Atlite presents  
 271 the best overall agreement with the observed frequency and duration of wind  
 272 drought events. This pattern is particularly evident for shorter-duration  
 273 events, which are the most frequent.

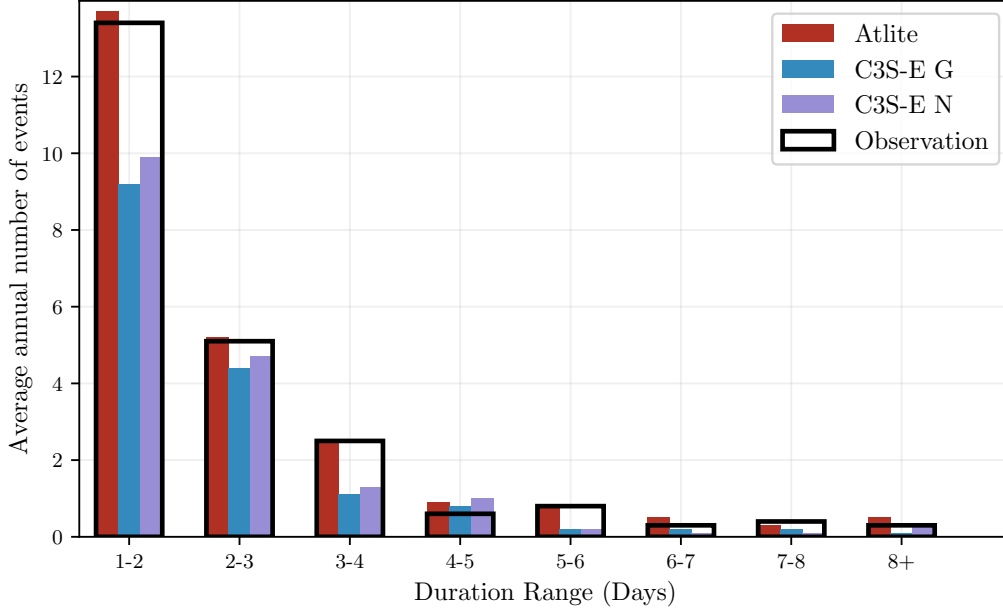


Figure 4: Average annual number of wind drought events for Atlite (red), C3S-E G (blue), C3S-E N (purple), and the observed data (black outline). The wind droughts are identified from 2014 to 2023, considering the actual capacity of the system at any given time

#### 274 4.1.2. Solar PV Energy

275 The Atlite model allows the user to select certain PV panel characteristics.  
 276 In this study, the three PV panel types available in the Atlite model were  
 277 considered (CSi, CdTe, Kaneka). Following the same methodology as in the  
 278 previous section, the three available models were compared using four skill  
 279 scores (CC, RMSE, MBE, and the percentage of overlap). Based on the best-  
 280 performing metrics, the Beyer PV panel model was selected [25], using the  
 281 Kaneka Hybrid panel option. For all solar PV farm locations, the azimuth  
 282 angle is fixed at 180°(due south), and the optimal tilt angle option is applied.

283 The solar PV installed capacity available on the spreadsheets from Eir-  
 284 Grid represents the Maximum Export Capacity (MEC) and does not ac-  
 285 curately reflect the installed solar PV capacity. To enable actual solar PV

286 generation potential to be modelled correctly, installed capacities were set at  
 287 1.4 times the MEC values. This scaling factor was estimated by analysing  
 288 proprietary data from individual solar PV farms provided by EirGrid, which  
 289 showed that, on average, assuming that the installed capacities of farms ex-  
 290 ceed their MEC values by 40% yields the best agreement with the observed  
 291 availability.

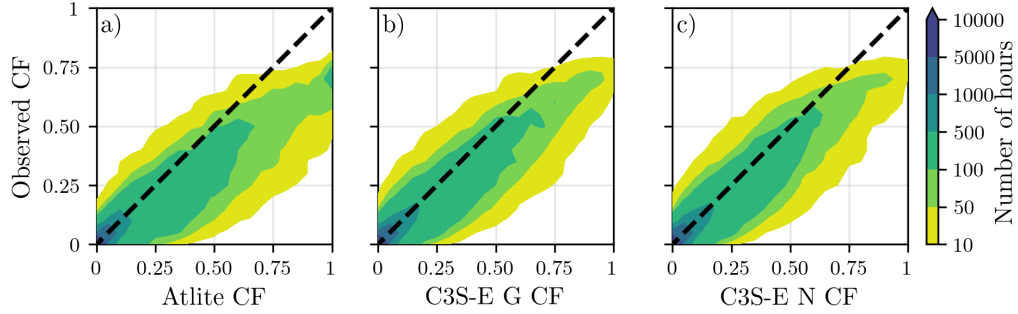


Figure 5: Solar PV CF density plot of the observed (vertical axes) and modelled (horizontal axes) CF series for the a) Atlite, b) C3S-E G and c) C3S-E N datasets

292 Figure 5 shows that the three datasets have a similar tendency to overesti-  
 293 mate the CF compared to the observed values, especially for high CF values.  
 294 The skill scores presented in Table 3 indicate that C3S-E G performs best  
 295 overall, with the lowest RMSE and a high correlation coefficient, suggesting  
 296 a closer match to observed data. All models show a slight positive bias, with  
 297 Atlite exhibiting a slightly lower correlation and higher RMSE.

	Atlite	C3S-E G	C3S-E N
<b>CC</b>	0.921	0.931	0.931
<b>RMSE</b>	0.119	0.090	0.113
<b>MBE</b>	0.046	0.027	0.021

Table 3: Skill scores for Solar PV CF for the three datasets compared to observed data

298 Fig. 6 shows the number of solar PV drought events during the 2023  
 299 validation period across different duration ranges. The figure reveals partial  
 300 agreement between the three datasets and the observed data, with consistent  
 301 results noticed for duration ranges of 1-2, 3-4, 7-8, and 8+ days. However,  
 302 discrepancies appear in the other ranges, where the models diverge from the

303 observed data. The main challenge in validating solar PV data stems from  
 304 the recent installation of a large share of Ireland’s PV capacity, with over  
 305 65% of the total PV capacity installed in 2023. This results in uncertainties  
 306 in PV generation data and the actual generating capacity in the first few  
 307 months after each farm is connected.

308 As the goal of this analysis is to assess the combination of wind and PV  
 309 generation, the complementary nature of these energy sources mitigates the  
 310 limitations in PV-only results.

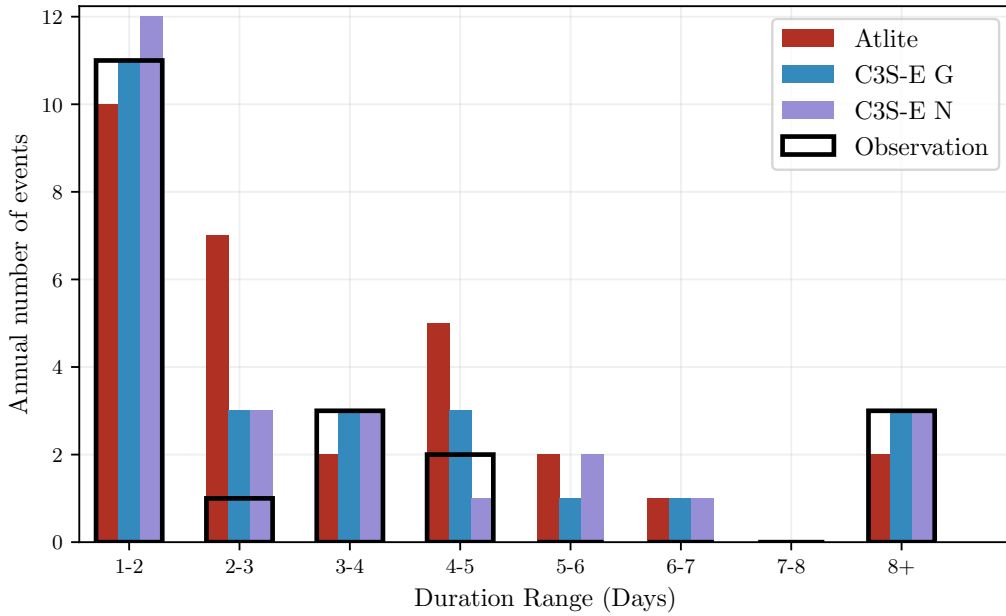


Figure 6: Number of PV drought events for Atlite (red), C3S-E G (blue), and C3S-E N (purple) and the observed data (black outline). The PV droughts are identified for 2023, considering the actual capacity of the system at any given time

#### 311 4.2. Analysis

312 In this section, RES drought events are evaluated under two different  
 313 scenarios with fixed installed capacities: the 91W-9PV scenario, with 5.9 GW  
 314 of wind capacity and 0.6 GW of PV capacity; and the 57W-43PV scenario,  
 315 where wind capacity comprises 11.45 GW and PV capacity increases to 8.6  
 316 GW. Both scenarios were driven by 45 years of ERA5 data. Using the RES  
 317 drought identification process described in Section 3.5, wind and PV droughts

are first analysed separately before presenting the results for combined (wind + PV) RES droughts under both scenarios.

It is important to note that this analysis is not focused on the absolute numbers characterizing RES droughts, but rather on the relative differences observed when comparing the various datasets and energy scenarios described in Section 3.4.

#### 4.2.1. Annual Number of RES Droughts

The analysis of annual RES drought events reveals trends that are largely consistent with earlier studies. When only wind energy is considered (Fig.7a), the number of drought events decreases as the duration range increases, with very few events lasting more than seven days. This pattern aligns with previous research showing that wind droughts tend to be short and frequent. In contrast, for PV energy (Fig.7b), drought frequency declines from one to eight days and then slightly increases for longer durations. This behaviour is attributable to Ireland’s high-latitude location, where reduced sunlight in winter (from November to March) leads to consistently low PV output.

Moreover, the comparison between wind and PV results indicates that the median, first, and third quartiles for PV are consistently higher than or equal to those for wind. This is expected, given that PV generation is inherently lower, zero at night, and limited by the solar cycle, as observed in other studies. When wind and PV are combined under the 91W-9PV scenario (Fig.7c), the results closely mirror those of wind alone, reaffirming wind’s dominance in the current energy mix. However, in the 57W-43PV scenario (Fig.7d), a marked reduction in drought events is observed across all datasets, with a decrease of the total number of events of 56% for Atlite, 52% for C3S-E G, and 50% for C3S-E N, demonstrating the beneficial effects of a more balanced energy mix. These findings are in line with earlier studies that highlight how increasing PV capacity can mitigate drought frequency through the anti-correlated seasonal patterns of wind and solar generation.

Additionally, the consistently higher drought counts reported by the Atlite dataset, compared to the C3S-E datasets, underscore the impact of model selection, particularly the influence of wind turbine power curve representation, on quantifying RES droughts. This observation is consistent with previous research, which has also noted that assumptions regarding turbine characteristics can significantly affect drought duration estimates.



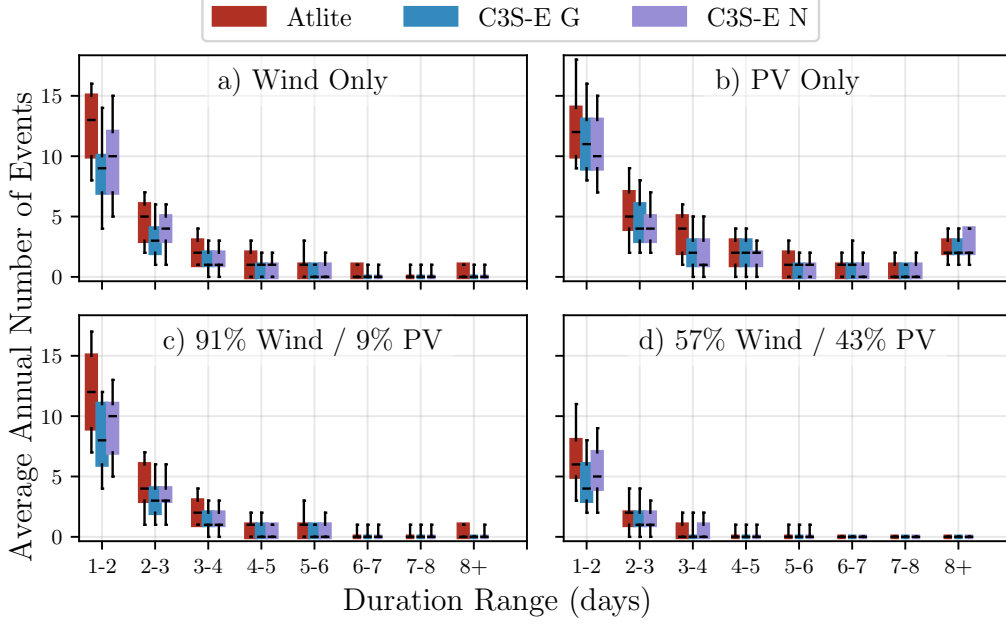


Figure 7: Average annual number of RES droughts (from 1979 to 2023) for a) Wind, b) PV, c) 91W-9PV and d) 57W-43PV for Atlite (red), C3S-E G (blue), and C3S-E N (purple). The x-axis represents duration ranges in days (lower bound included), while the y-axis indicates the annual number of events. The boxes display the first and third quartiles and the median is marked by a black line. The whiskers indicate the 5th and 95th percentiles

#### 4.2.2. Return Periods of RES Drought Duration

The RES drought events identified over the 45-year period were used to calculate the return periods for different RES drought durations. A return period is the estimated average time interval between events of a specified duration or intensity (not to be confused with the frequency of their occurrence within a fixed time frame). Fig. 8 illustrates the return periods for varying RES drought durations, highlighting how often different drought lengths are likely to occur across the datasets. This analysis provides insight into the frequency and likelihood of prolonged low-generation periods, which is crucial for evaluating the impact of extreme RES droughts on system resilience. Understanding these return periods is essential, as even infrequent can challenge energy security by placing significant strain on conventional backup sources necessary to maintain supply in high-RES scenarios.

For wind (Fig. 8a), the log-linear increase in return periods observed in

367 this study confirms that longer droughts occur exponentially less frequently,  
 368 a trend consistent with earlier research on wind variability. In the case of  
 369 PV droughts (Fig. 8b), the Atlite dataset shows a generally log-linear trend,  
 370 while the C3S-E datasets exhibit a sudden increase in drought duration for  
 371 events exceeding sixteen days. This abrupt rise reflects differences in how PV  
 372 output is handled near the CF threshold during low irradiance conditions.  
 373 Interestingly, when the share of wind power is decreased in the balanced  
 374 scenario, the overall return periods for drought events increase. Although  
 375 wind energy is generally more stable, reducing its share makes the combined  
 376 system more vulnerable to PV's extended low-generation periods in winter.  
 377 This highlights that the seasonal limitations of PV can dominate the overall  
 378 drought characteristics when its share increases, emphasizing the importance  
 379 of carefully balancing the energy mix for RES drought risk assessment.

380 Under the 91W-9PV scenario (Fig. 8c), the combined RES drought return  
 381 periods largely mirror those for wind alone, reflecting the dominance of wind  
 382 in the current energy mix. In contrast, the balanced 57W-43PV scenario  
 383 (Fig. 8d) shows a dramatic increase in return periods across all durations,  
 384 suggesting that a more diversified energy mix can substantially mitigate the  
 385 frequency of prolonged drought events.

386 Across Fig. 8a, c, and, d, the return periods in the Atlite dataset are con-  
 387 sistently higher than those in the two C3S-E datasets. For instance, in the  
 388 91W-9PV scenario (Fig. 8c), an event with a one-year return period lasts six  
 389 days in the Atlite dataset, compared to only five days in the C3S-E datasets.  
 390 This difference underscores the importance of model selection when quan-  
 391 tifying RES droughts, as each dataset's assumptions and parametrisations  
 392 significantly influence drought duration estimates. Additionally, in all four  
 393 graphs, the similarity between results from the two C3S-E datasets suggests  
 394 that assumptions in the Atlite dataset, such as wind turbine power curve  
 395 selection and PV panel specifications, have a greater impact on RES drought  
 396 duration estimates than the precise geographic distribution of RES farms  
 397 when studying the return periods of RES droughts.

#### 398 *4.2.3. Seasonal Distribution of RES Droughts*

399 The seasonal analysis of RES droughts is based on the percentage of hours  
 400 in each month classified as drought events. Wind droughts tend to be more  
 401 frequent during summer, whereas PV droughts are more common in winter  
 402 due to reduced sunlight. By comparing these seasonal patterns across dif-  
 403 ferent datasets and energy scenarios, the study examines how model-specific

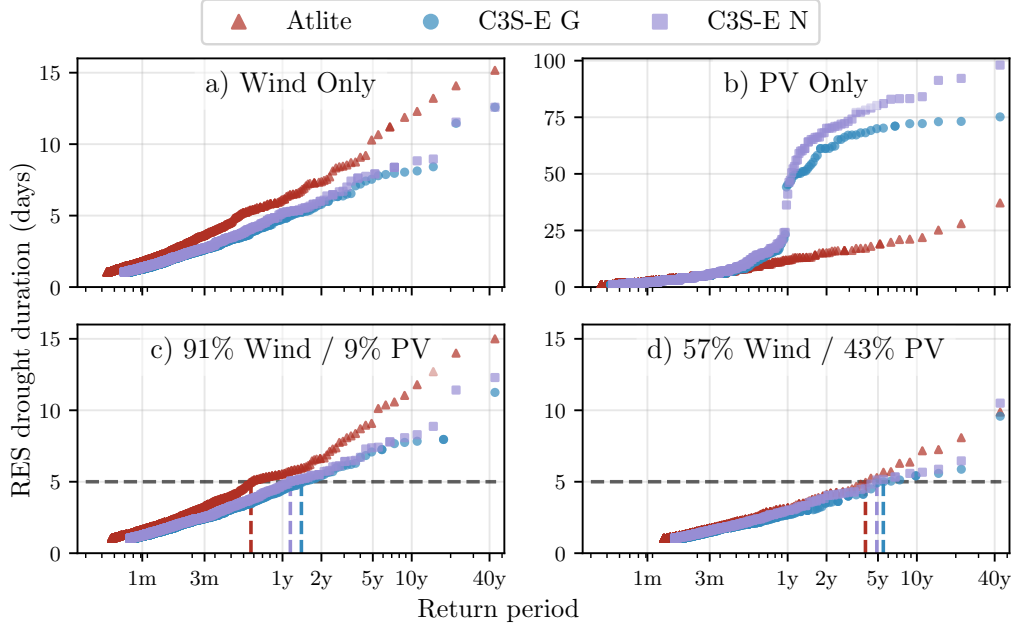


Figure 8: Return periods of the duration of RES droughts (from 1979 to 2023) for a) Wind, b) PV, c) 91W-9PV and d) 57W-43PV for Atlite (red triangle), C3S-E G (blue circle), and C3S-E N (purple square). The x-axis represents the return period time in a log-scale and the y-axis indicates the duration of RES drought associated with it. The horizontal dashed line marks the 5-day return period, with coloured vertical dashed marking its return period for each dataset

assumptions and variations in capacity mix affect the overall characterisation of drought events.

For the wind-only scenario (Fig. 9a), the Atlite dataset exhibits a pronounced seasonal pattern, with about 24% of summer hours (June–July–August) identified as droughts compared to only 4% in winter (December–January–February). This strong seasonal signal is less evident in the C3S-E datasets, which suggests that the differences in the underlying wind power curves play a significant role. In Atlite, CF near or below the 0.1 threshold occurs at relatively higher wind speeds, resulting in a higher count of drought hours during the summer months.

In contrast, PV droughts (Fig. 9b) display an opposite seasonal trend. Across all datasets, over 60% of winter hours are classified as PV droughts, reflecting the naturally low solar irradiance in Ireland during winter. More-

over, Atlite tends to record a slightly higher percentage of drought hours for wind and a marginally lower percentage for PV relative to the C3S-E datasets. These differences highlight how dataset-specific assumptions, such as the treatment of wind turbine power curves and PV panel characteristics, significantly influences the apparent seasonal dynamics of RES droughts.

The 91W-9PV scenario (Fig. 9c) shows patterns comparable to the ones for wind droughts (Fig. 9a). However, in the 91W/9PV scenario, the number of hours classified as RES droughts in summer decreases slightly compared to the wind-only scenario. This reduction can be explained by the contribution of PV generation during the summer months in the 91W-9PV scenario, even though it constitutes only 11% of total capacity. Since the number of RES drought hours for PV in summer is near zero, this small contribution has a noticeable impact on reducing overall drought hours. In the 57W-43PV scenario (Fig. 9d), all three datasets show a reduction in monthly RES drought frequency. Annual reductions in median RES drought frequency are observed across the datasets, dropping from 14% to 5% for Atlite, from 8% to 3% for C3S-E G, and from 9% to 4% for C3S-E N. The balanced mix of wind and PV power in this scenario reduces the seasonal signal overall and significantly decreases the percentage of RES drought hours in the summer.

The seasonal variations observed in this study have important implications for energy planning. Given that energy demand peaks in winter for Northern European countries, understanding these seasonal patterns is critical for assessing the need for conventional backup or storage solutions during periods of prolonged low renewable output. The findings underscore that even small differences in model assumptions leads to significant variations in drought estimates, thereby affecting the reliability of the energy system during critical periods. Such insights are essential for policymakers to develop targeted strategies that enhance grid resilience and ensure a stable energy supply throughout the year.

## 5. Conclusions

This study has investigated the ability of three RES datasets to represent RES droughts: Atlite, C3S-E G, and C3S-E N. One of the most evident differences is how each dataset incorporates the specific locations of RES farms. Both Atlite and C3S-E G consider the locations of wind and PV farms, which one would expect to result in a more accurate representation of RES generation. While this approach slightly improves PV models, our

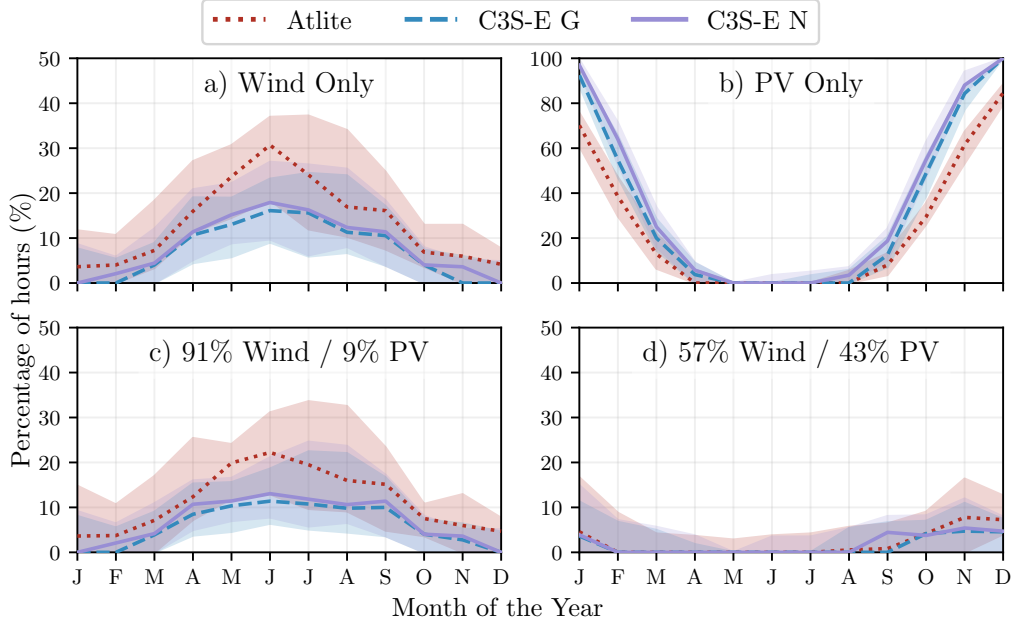


Figure 9: Percentage of hours in a month which are part of a RES drought (from 1979 to 2023) for a) Wind, b) PV, c) 91W-9PV and d) 57W-43PV for Atlite (red dotted), C3S-E G (blue dashed), and C3S-E N (purple solid). The x-axis represents the month of the year, and the y-axis indicates the percentage of hours. Lines correspond to the median values and the area between the first and third quartiles is shaded. Note the different y-axis scale for b).

analysis indicates that for wind energy, the Atlite dataset performs better overall, especially in its close alignment with observed data for wind generation estimates. This finding suggests that, although the inclusion of RES farm locations is beneficial, the accuracy of the RES dataset is more strongly influenced by underlying model assumptions, such as selecting an appropriate wind power curve.

Atlite shows the best alignment with observed data for wind generation. Differences between the datasets are smaller for PV, with C3S-G performing marginally better than the other two. The results show that the two C3S-E datasets (C3S-E G and C3S-E N) consistently yield similar outcomes, indicating that their methodological differences have minimal impact in this case. This distinction is also evident in the analysis, where Atlite reports higher return periods and a greater number of RES droughts, especially in

466 scenarios with a balanced share of RES. Again, the results from RES drought  
467 modelling rely more on the precision of the wind power curve and PV panel  
468 models than on the specific locations of RES farms. Atlite’s superior perfor-  
469 mance highlights the importance of selecting validated models for assessing  
470 RES drought risks. This careful model selection can better quantify risks,  
471 support effective planning, and avoid the potential underestimation of ca-  
472 pacity needs, which is essential for ensuring energy security.

473 Looking at the 57W-43PV scenario, the analysis showed a significant im-  
474 provement in the management of RES droughts due to the complementary  
475 nature of wind and PV generation. Wind and PV together perform better  
476 in terms of reducing drought frequency and duration than either would in-  
477 dividually, largely because of the seasonal anti-correlation between the two  
478 energy sources. This diversification reduces the seasonal impact on RES  
479 droughts, as PV generation peaks in the summer and wind generation is  
480 more consistent in winter. Ireland currently has a highly wind-dependent  
481 energy system, but with ambitious targets for PV installations in the coming  
482 years, the energy mix is expected to approach a balance between wind and  
483 PV capacity. While this balanced approach offers a more stable and secure  
484 energy supply by mitigating RES drought risks, it is important to note that  
485 having similar wind and PV capacities may not optimise other aspects, such  
486 as annual energy production or meeting nighttime loads. For policymakers,  
487 these findings underscore the importance of meeting these capacity targets  
488 to enhance energy security through diversification. Additionally, the choice  
489 of model for RES drought assessment becomes increasingly critical as more  
490 renewable capacity is integrated into the system.

491 This study has several limitations. Although ERA5 is among the best  
492 reanalysis datasets for renewable energy analysis [? ] ?, its resolution may  
493 not capture local-scale phenomena, making it less reliable at the individual  
494 farm level. In addition, our methodology employs a fixed threshold to define  
495 RES drought events, which is necessary to compare the three models but  
496 does not account for demand variations. Consequently, while this approach  
497 enables a consistent inter-comparison, it may overlook events that are most  
498 critical for power system operations.

499 Future work is planned to extend the current analysis. First, climate  
500 projection data will be integrated with different energy scenarios, incorpo-  
501 rating the addition of offshore wind, to better understand how climate change  
502 might affect RES droughts. Second, expanding the geographic domain of the  
503 study to include the rest of Europe would provide a more comprehensive un-

derstanding of RES droughts in an interconnected energy grid. This would require extensive verification across other European countries, making it a more complex but highly relevant challenge.

## Data Availability

The ERA5 data can be obtained from the Climate Data Store (<https://doi.org/10.24381/cds.adbb2d47>). The C3S-E dataset is also available from the Climate Data Store (<https://doi.org/10.24381/cds.4bd77450>). Information on wind and PV farms in Ireland can be obtained from the EirGrid website (<https://www.eirgrid.ie/grid/system-and-renewable-data-reports>). The Atlite model used in this study is open-source and can be found on GitHub (<https://github.com/pypsa/atlite>). The data and code required to reproduce the analysis in this article will be made available upon acceptance of the manuscript in a public GitHub repository.

## Acknowledgments

The research conducted in this publication was funded by Science Foundation Ireland and co-funding partners under grant number 21/SPP/3756 through the NexSys Strategic Partnership Programme.

## References

- [1] EuroStat, Renewable Energy Statistics, 2023. URL: [https://ec.europa.eu/eurostat/statistics-explained/index.php?title=Renewable\\_energy\\_statistics](https://ec.europa.eu/eurostat/statistics-explained/index.php?title=Renewable_energy_statistics), Accessed: 2024-11-06.
- [2] H. C. Bloomfield, D. J. Brayshaw, L. C. Shaffrey, P. J. Coker, H. E. Thornton, Quantifying the increasing sensitivity of power systems to climate variability, *Environmental Research Letters* 11 (2016) 124025. doi:10.1088/1748-9326/11/12/124025.
- [3] H. C. Bloomfield, D. J. Brayshaw, A. Troccoli, C. M. Goodess, M. De Felice, L. Dubus, P. E. Bett, Y.-M. Saint-Drenan, Quantifying the sensitivity of european power systems to energy scenarios and climate change projections, *Renewable Energy* 164 (2021) 1062–1075. doi:10.1016/j.renene.2020.09.125.

- [4] F. Kaspar, M. Borsche, U. Pfeifroth, J. Trentmann, J. Drücke, P. Becker, A climatological assessment of balancing effects and shortfall risks of photovoltaics and wind energy in germany and europe, *Advances in Science and Research* 16 (2019) 119–128. doi:10.5194/asr-16-119-2019.
- [5] F. Mockert, C. M. Grams, T. Brown, F. Neumann, Meteorological conditions during periods of low wind speed and insolation in Germany: The role of weather regimes, *Meteorological Applications* 30 (2023) e2141. doi:10.1002/met.2141.
- [6] M. Ohba, Y. Kanno, D. Nohara, Climatology of dark doldrums in japan, *Renewable and Sustainable Energy Reviews* 155 (2022) 111927. doi:10.1016/j.rser.2021.111927.
- [7] M. J. Mayer, B. Biró, B. Szücs, A. Aszódi, Probabilistic modeling of future electricity systems with high renewable energy penetration using machine learning, *Applied Energy* 336 (2023) 120801. doi:10.1016/j.apenergy.2023.120801.
- [8] D. Raynaud, B. Hingray, B. François, J. Creutin, Energy droughts from variable renewable energy sources in European climates, *Renewable Energy* 125 (2018) 578–589. doi:https://doi.org/10.1016/j.renene.2018.02.130.
- [9] A. Gangopadhyay, A. K. Seshadri, N. J. Sparks, R. Toumi, The role of wind-solar hybrid plants in mitigating renewable energy-droughts, *Renewable Energy* 194 (2022) 926–937. doi:10.1016/j.renene.2022.05.122.
- [10] J. Kapica, J. Jurasz, F. A. Canales, H. Bloomfield, M. Guezgouz, M. De Felice, Z. Kobus, The potential impact of climate change on european renewable energy droughts, *Renewable and Sustainable Energy Reviews* 189 (2024) 114011. doi:10.1016/j.rser.2023.114011.
- [11] K. Z. Rinaldi, J. A. Dowling, T. H. Ruggles, K. Caldeira, N. S. Lewis, Wind and Solar Resource Droughts in California Highlight the Benefits of Long-Term Storage and Integration with the Western Interconnect, *Environmental Science and Technology* 55 (2021) 6214–6226. doi:10.1021/acs.est.0c07848.



- [12] P. T. Brown, D. J. Farnham, K. Caldeira, Meteorology and climatology of historical weekly wind and solar power resource droughts over western North America in ERA5, *SN Applied Sciences* 3 (2021) 814. doi:10.1007/s42452-021-04794-z.
- [13] S. Allen, N. Otero, Standardised indices to monitor energy droughts, *Renewable Energy* 217 (2023) 119206. doi:10.1016/j.renene.2023.119206.
- [14] C. Bracken, N. Voisin, C. D. Burleyson, A. M. Campbell, Z. J. Hou, D. Broman, Standardized benchmark of historical compound wind and solar energy droughts across the Continental United States, *Renewable Energy* 220 (2024) 119550. doi:https://doi.org/10.1016/j.renene.2023.119550.
- [15] H. Lei, P. Liu, Q. Cheng, H. Xu, W. Liu, Y. Zheng, X. Chen, Y. Zhou, Frequency, duration, severity of energy drought and its propagation in hydro-wind-photovoltaic complementary systems, *Renewable Energy* (2024) 120845. doi:10.1016/j.renene.2024.120845, 2.
- [16] H. Hersbach, B. Bell, P. Berrisford, S. Hirahara, A. Horányi, J. Muñoz-Sabater, J. Nicolas, C. Peubey, R. Radu, D. Schepers, et al., The ERA5 global reanalysis, *Quarterly Journal of the Royal Meteorological Society* 146 (2020) 1999–2049. doi:10.1002/qj.3803.
- [17] L. Dubus, Y. Saint-Drenan, A. Troccoli, M. De Felice, Y. Moreau, L. Ho-Tran, C. Goodess, R. Amaro E Silva, L. Sanger, C3S Energy: A climate service for the provision of power supply and demand indicators for Europe based on the ERA5 reanalysis and ENTSO-E data, *Meteorological Applications* 30 (2023) e2145. doi:10.1002/met.2145.
- [18] F. Hofmann, J. Hampp, F. Neumann, T. Brown, J. Hörsch, Atlite: a lightweight Python package for calculating renewable power potentials and time series, *Journal of Open Source Software* 6 (2021) 3294. doi:10.21105/joss.03294.
- [19] EirGrid & SONI, System and Renewable Data Reports, 2023. URL: <https://www.eirgrid.ie/grid/system-and-renewable-data-reports>, Accessed: 2024-11-06.

- 599 [20] E. Doddy Clarke, S. Griffin, F. McDermott, J. Monteiro Correia,  
600 C. Sweeney, Which reanalysis dataset should we use for renewable en-  
601 ergy analysis in ireland?, *Atmosphere* 12 (2021) 624. doi:10.3390/atmo-  
602 s12050624.
- 603 [21] Y.-M. Saint-Drenan, L. Wald, T. Ranchin, L. Dubus, A. Troccoli, An  
604 approach for the estimation of the aggregated photovoltaic power gener-  
605 ated in several European countries from meteorological data, *Advances*  
606 *in Science and Research* 15 (2018) 51–62. doi:10.5194/asr-15-51-201-  
607 8.
- 608 [22] I. Staffell, S. Pfenninger, Using bias-corrected reanalysis to simulate  
609 current and future wind power output, *Energy* 114 (2016) 1224–1239.  
610 doi:10.1016/j.energy.2016.08.068.
- 611 [23] Government of Ireland, Climate Action Plan 2024, Technical Report 3,  
612 Department of the Environment, Climate and Communications, 2023.  
613 URL: [https://www.gov.ie/pdf/?file=https://assets.gov.ie/](https://www.gov.ie/pdf/?file=https://assets.gov.ie/284675/70922dc5-1480-4c2e-830e-295afd0b5356.pdf)  
614 [284675/70922dc5-1480-4c2e-830e-295afd0b5356.pdf](https://assets.gov.ie/284675/70922dc5-1480-4c2e-830e-295afd0b5356.pdf), Accessed:  
615 2024-11-06.
- 616 [24] Sustainable Energy Authority Ireland, National Energy Projections  
617 2024, Technical Report, Sustainability Energy Authority of Ireland,  
618 2024. URL: [https://www.seai.ie/news-and-events/news/energ](https://www.seai.ie/news-and-events/news/energy-projections-report)  
619 [y-projections-report](https://www.seai.ie/news-and-events/news/energy-projections-report), Accessed: 2024-11-06.
- 620 [25] H. G. Beyer, G. Heilscher, S. Bofinger, A robust model for the mpp  
621 performance of different types of pv-modules applied for the performance  
622 check of grid connected systems, *Eurosun* (2004) 8.